A LETTERS JOURNAL EXPLORING THE FRONTIERS OF PHYSICS

OFFPRINT

Fine structure of ^{211}Bi α-decay from Coriolis coupling

M. MIREA

EPL, **124** (2018) 12001

epl

A Letters Journal Exploring the Frontiers of Physics

AN INVITATION TO SUBMIT YOUR WORK

epljournal.org

The Editorial Board invites you to submit your Letters to EPL

Choose EPL, and you'll be published alongside original, innovative Letters in all areas of physics. The broad scope of the journal means your work will be read by researchers in a variety of fields; from condensed matter, to statistical physics, plasma and fusion sciences, astrophysics, and more.

Not only that, but your work will be accessible immediately in over 3,300 institutions worldwide. And thanks to EPL's green open access policy you can make it available to everyone on your institutional repository after just 12 months.

Run by active scientists, for scientists

Your work will be read by a member of our active and international Editorial Board, led by Bart Van Tiggelen. Plus, any profits made by EPL go back into the societies that own it, meaning your work will support outreach, education, and innovation in physics worldwide.

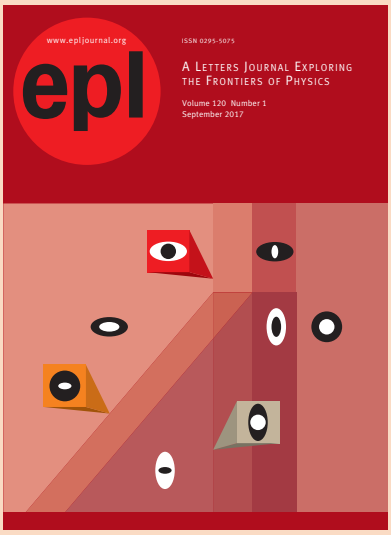

OVER

638,000

full-text downloads in 2017

Average submission to online publication

100 DAYS

21,500

citations in 2016

We greatly appreciate the efficient, professional and rapid processing of our paper by your team.

Cong Lin
Shanghai University

Four good reasons to publish with EPL

1. **International reach** – more than 3,300 institutions have access to EPL globally, enabling your work to be read by your peers in more than 90 countries.

2. **Exceptional peer review** – your paper will be handled by one of the 60+ co-editors, who are experts in their fields. They oversee the entire peer-review process, from selection of the referees to making all final acceptance decisions.

3. **Fast publication** – you will receive a quick and efficient service; the median time from submission to acceptance is 75 days, with an additional 20 days from acceptance to online publication.

4. **Green and gold open access** – your Letter in EPL will be published on a green open access basis. If you are required to publish using gold open access, we also offer this service for a one-off author payment. The Article Processing Charge (APC) is currently €1,400.

Details on preparing, submitting and tracking the progress of your manuscript from submission to acceptance are available on the EPL submission website, **epletters.net**.

If you would like further information about our author service or EPL in general, please visit **epljournal.org** or e-mail us at **info@epljournal.org**.

EPL is published in partnership with:

European Physical Society

Società Italiana di Fisica

EDP Sciences

IOP Publishing

A Letters Journal Exploring the Frontiers of Physics

October 2018

EPL, **124** (2018) 12001 www.epljournal.org
doi: 10.1209/0295-5075/124/12001

Fine structure of ^{211}Bi α-decay from Coriolis coupling

M. Mirea

Horia Hulubei National Institute for Physics and Nuclear Engineering - P.O. Box MG-6, Bucharest-Magurele, Romania,
Academy of Romanian Scientists - Splaiul Independentei 54, 050094, Bucharest, Romania and
Faculty of Physics, University of Bucharest - Atomistilor Street 405, Bucharest-Magurele, Romania

received 13 August 2018; accepted in final form 4 October 2018
published online 5 November 2018

PACS 23.60.+e – α decay
PACS 24.10.Eq – Coupled-channel and distrorded-wave models
PACS 21.60.Cs – Shell model

Abstract – The α-decay is considered as a superasymmetric fission process. A fragmentation path is obtained by mean of the least action principle in a configuration space spanned by five degrees of freedom. The potential barrier is obtained within the macroscopic-microscopic model while the effective mass and the momentum of inertia within the cranking approach. The single-particle wave functions and the single-particle energies are supplied by the Woods-Saxon two-center shell model. The fine structure of ^{211}Bi α-decay is treated within a set of generalized time-dependent pairing equations that takes into account the Landau-Zener effect and the Coriolis coupling. A low value of the internuclear collective velocity was used. The theoretical results showed a good agreement with the experimental data. Essentially, in the framework of the formalism, the fine structure for the ^{211}Bi is due to the occurrence of the Coriolis coupling.

Introduction. – The classical phenomenology of α-decay assumes that a preformed cluster penetrates an external potential barrier, essentially of Coulomb nature [1]. The probability of the formation of the α-particle is known as spectroscopic factor, and it is calculated as an overlap of the state of the initial fragment nucleus and that of the system formed by the daughter and the alpha cluster at scission [2,3]. The way in which the α-particle appears on the surface of the nucleus is still a subject of investigations [4–7]. However, in the classical α-decay theory only the initial and the final states should be known. The half-life of the process is mainly ruled by the Q-value of the reaction that fixes the height of the potential barrier. The fine structure of α-radioactivity means that the emission probability depends on the final state of the daughter. The theory of the fine structure of α-decay has been reviewed recently in ref. [8]. In the current theory, the fine structure is evaluated with a time-independent system of coupled channels equations for the α-daughter radial motion.

In the following, the α-emission is treated with a fission-like formalism. In the spontaneous-fission theory, firstly we need to determine a fragmentation path that starts from the ground state of the parent nucleus and arrives in the scission point. This path in obtained within the least action principle, by taking into account the variation of two quantities: the potential energy and the inertia. Both ingredients depend on the rearrangement of the nuclear structure during the deformation, while the inertia depends also on the history of the evolution of the nuclear system. In principle, the fission model should not need the knowledge of empirical parameters as the Q-value, because the collective potential should reproduce the ground-state mass of the parent in the initial state and those of the daughter and of the α-particle in the asymptotic configuration. Recently, the ^{211}Po α-decay fine structure was investigated as solution of a system of microscopic equations of motion [9], by considering the α-decay as a superasymmetric fission process. This system takes into account dynamical and microscopical effects. It was shown that excitations on superior single-particle levels of the ^{207}Pb daughter nucleus are mainly due to the Landau-Zener effect. This effect is due to the rearrangement in time of the nuclear structure. It was predicted that a similar effect should be responsible for the fine structure of the ^{211}Bi α-decay, due to a possible existence of an avoided crossing region located in the Fermi energy gap region. In the following, the fission approach is used to describe the fine structure of the α-decay ^{211}Bi. In this study, the importance of the Coriolis coupling produced during the formation of the α-cluster is emphasized.

Microscopic equations of motion. – The microscopic equations of motion deduced in ref. [9] are used to determine the spectroscopic factors. These equations are obtained from the variation of the energy functional

$$\delta L = \delta\Big\langle \varphi_{IM}\Big| H + H_R - i\frac{\partial}{\partial t} + H' - \lambda|N_2\hat{N}_1 - N_1\hat{N}_2|\Big|\varphi_{IM}\Big\rangle \quad (1)$$

where H is the many-body Hamiltonian with pairing residual interaction:

$$H = \sum_{\Omega,m}\epsilon_{\Omega,m}\left(a^+_{\Omega,m}a_{\Omega,m} + a^+_{\bar{\Omega},m}a_{\bar{\Omega},m}\right) - G\sum_{(\Omega,m)(\Omega_1,m_1)} a^+_{\Omega,m}a^+_{\bar{\Omega},m}a_{\Omega_1,m_1}a_{\bar{\Omega}_1,m_1}. \quad (2)$$

One denoted with $\epsilon_{\Omega,m}$ the single-particle energies, and with G a constant pairing interaction. The symbol $\epsilon_{\Omega,m}$ means the single-particle states m with the projection of the spin Ω, while $a^+_{\Omega,m}/a_{\Omega,m}$ are the single-particle creation/annihilation operators, In the functional (1), H' denotes an interaction that is responsible for the nucleon promotion mechanism between single-particles states characterized by the same good quantum numbers, generically known as the Landau-Zener effect [10,11]:

$$H' = \sum_{\Omega,m,m'} h_{\Omega,m,m'}\alpha^+_{\Omega,m'(\Omega,m')}\alpha_{\Omega,m'(\Omega,m)} \times \prod_{\Omega',m''}\alpha_{\Omega',m''(\Omega,m')}a^+_{\Omega',m''}a_{\Omega',m''}\alpha^+_{\Omega',m''(\Omega,m)}, \quad (3)$$

where $\alpha^+_{\Omega,m'(\Omega,m')} = u_{\Omega,m(\Omega,m')}a^+_{\Omega,m} - v^*_{\Omega,m(\Omega,m')}a_{\bar{\Omega},m}$ is the quasiparticle creation operator and $\alpha_{\Omega,m'(\Omega,m)} = u_{\Omega,m'(\Omega,m)}a_{\Omega,m'} - v_{\Omega,m'(\Omega,m)}a^+_{\bar{\Omega},m'}$ is the quasiparticle annihilation operator. Here, $h_{\Omega,m,m'}$ is the interaction energy between states m and m', in the avoided crossing level regions. If the nuclear shape parametrization is axial symmetric, the good quantum numbers are the projection of the intrinsic spin Ω on the axis of symmetry. The symbols $u_{\Omega,m'(\Omega,m)}$ and $v_{\Omega,m'(\Omega,m)}$ are the BCS amplitudes of the single-particle level (Ω,m') in the seniority-one configuration (Ω,m). The term (3) is discussed in ref. [12], where a generalization of the pairing equations of motion by including the Landau-Zener effect was realized. This term is also responsible for a dynamical pair breaking mechanism [13]. The axial symmetric rotor energy is [14]

$$H_R = \frac{\hbar^2}{2J}\left(I^2 - j_z^2\right) + \frac{\hbar^2}{2J}\left(j_x^2 + j_y^2\right) - \frac{\hbar^2}{2J}\left(j_+I_- + j_-I_+\right), \quad (4)$$

where J denotes the total momentum of inertia, $I = (I_x, I_y, I_z)$ represents the total angular momentum and $j = (j_x, j_y, j_z)$ is the intrinsic angular momentum of a particle. Finally, the dynamical condition for the projection of the number of particles in the final fragments appearing in formula (1) is obtained with the supplementary condition $|N_2\hat{N}_1 - N_1\hat{N}_2|$, as discussed in refs. [15,16]. So, $\hat{N}_1$ and $\hat{N}_2$ are particle number operators associated to the final fragments, while λ is a Lagrange multiplier. The trial many body-state is considered as a superposition of products between seniority-one Bogoliubov wave functions and rotation functions:

$$|\varphi_{IM}\rangle = \sum_{\Omega,m} c_{\Omega,m}|\varphi_{IM\Omega m}\rangle = \sum_{\Omega,m} c_{\Omega,m}b^+_{I,M,\Omega,m}\prod_{(\Omega_1,m_1)\neq(\Omega,m)} \times\left(u_{\Omega_1,m_1(\Omega,m)} + v_{\Omega_1,m_1(\Omega,m)}a^+_{\Omega_1,m_1}a^+_{\bar{\Omega}_1,m_1}\right)|0\rangle \quad (5)$$

with

$$b^+_{I,M,\Omega,m}|0\rangle = \left(\frac{2I+1}{8\pi^2}\right)^{1/2}\left(\frac{\Omega}{|\Omega|}\right)^{I+\Omega}\mathcal{D}^I_{M\Omega}(\omega)a^+_{\Omega,m}|0\rangle, \quad (6)$$

where Ω represents the intrinsic spin projection on the axis of symmetry. As mentioned, m identifies different states in the same Ω levels space. Here, $\mathcal{D}^I_{M\Omega}(\omega)$ denotes the rotation function, while $c_{\Omega,m}$ are the amplitudes of different seniority-one configurations. Therefore, $|c_{\Omega,m}|^2$ is the probability to find the seniority-one configuration with the unpaired nucleon located on the single-particle level labeled by the quantum numbers (Ω,m).

As detailed in ref. [9], the next time-dependent equations of motion emerge:

$$\begin{aligned}
&-i\hbar\dot{c}^*_{\Omega,m} = \\
&c^*_{\Omega,m}\Bigg\{2\sum_{(\Omega',m')\neq(\Omega,m)} |\, v_{\Omega',m'(\Omega,m)}\,|^2\,(\epsilon_{\Omega',m'} - \lambda) \\
&+ (\epsilon_{\Omega,m} - s_k\lambda N_k) \\
&- G\Bigg|\sum_{(\Omega'm')\neq(\Omega,m)} u_{\Omega',m'(\Omega,m)}v_{\Omega',m'(\Omega,m)}\Bigg|^2 \\
&- G\sum_{(\Omega',m')\neq(\Omega,m)} |\, v_{\Omega',m'(\Omega,m)}\,|^4\Bigg\} \\
&+ \frac{\hbar^2}{2J}c^*_{\Omega,m}[I(I+1) - \Omega^2] \\
&- \frac{\hbar^2}{2J}\Bigg\{\sum_{m'} c^*_{\Omega+1,m'}((I-\Omega)(I+\Omega+1))^{1/2} \\
&\times [u_{\Omega,m(\Omega+1,m')}u_{\Omega+1,m'(\Omega,m)} \\
&+ v^*_{\Omega,m(\Omega+1,m')}v_{\Omega+1,m'(\Omega,m)}] \\
&\times \langle\Omega+1,m'|j_+|\Omega,m\rangle T_{\Omega+1,m',\Omega,m} \\
&+ \sum_{m'} c^*_{\Omega-1,m'}((I+\Omega)(I-\Omega+1))^{1/2} \\
&\times [u_{\Omega,m(\Omega-1,m')}u_{\Omega-1,m'(\Omega,m)} \\
&+ v^*_{\Omega,m(\Omega-1,m')}v_{\Omega-1,m'(\Omega,m)}]
\end{aligned}$$

$$\times \langle \Omega - 1, m' | j_- | \Omega, m \rangle T_{\Omega-1,m',\Omega,m} \}$$
$$- i\hbar c^*_{\Omega,m} \sum_{(\Omega',m') \neq (\Omega,m)} \frac{1}{2} (v^*_{\Omega',m'(\Omega,m)} \dot{v}_{\Omega',m'(\Omega,m)}$$
$$- \dot{v}^*_{\Omega' m'(\Omega,m)} v_{\Omega',m'(\Omega,m)})$$
$$+ \sum_{m' \neq m} h_{\Omega,m',m} c^*_{\Omega,m'} T_{\Omega,m',\Omega,m}, \quad (7)$$

where the parameter $s_k = \pm 1$ ensures a positive value for the condition of dynamical projection on the numbers of particles in both fragments at scission introduced through the Lagrange multiplier λ in the functional (1). The number of nucleons in the fragment k is N_k. A shorthand notation is used for the overlaps of products of quasiparticle wave functions,

$$T_{\Omega',m',\Omega,m} =$$
$$\left\langle 0 \right| \prod_{\Omega_1,m_1} (u_{\Omega_1,m_1(\Omega',m')} + v_{\Omega_1,m_1(\Omega',m')} a^+_{\Omega_1,m_1} a^+_{\bar{\Omega}_1,m_1})$$
$$\times \left| \prod_{\Omega_2,m_2} (u_{\Omega_2,m_2(\Omega,m)} + v_{\Omega_2,m_2(\Omega,m)} a^+_{\Omega_2,m_2} a^+_{\bar{\Omega}_2,m_2}) \right| 0 \right\rangle$$
$$= \prod_{\Omega_1,m_1} [u_{\Omega_1,m_1(\Omega',m')} u_{\Omega_1,m_1(\Omega,m)}$$
$$+ v^*_{\Omega_1,m_1(\Omega',m')} v_{\Omega_1,m_1(\Omega,m)}]. \quad (8)$$

After manipulating the time-dependent pairing equations [17,18], the time derivatives $\dot{v}_{\Omega',m'(\Omega,m)}$ are given by

$$\frac{i\hbar}{2} (v^*_{\Omega',m'(\Omega,m)} \dot{v}_{\Omega',m'(\Omega,m)} - \dot{v}^*_{\Omega',m'(\Omega,m)} v_{\Omega',m'(\Omega,m)}) =$$
$$2 \mid v_{\Omega',m'(\Omega,m)} \mid^2 (\epsilon_{\Omega',m'} - \lambda) - 2G \mid v_{\Omega',m'(\Omega,m)} \mid^4$$
$$+ \Re \Big\{ \Delta^*_{\Omega,m} \Big(\frac{\mid v_{\Omega',m'(\Omega,m)} \mid^4}{u_{\Omega',m'(\Omega,m)} v^*_{\Omega',m'(\Omega,m)}}$$
$$- u_{\Omega',m'(\Omega,m)} v_{\Omega',m'(\Omega,m)} \Big) \Big\} \quad (9)$$

and the system becomes tractable. As demonstrated in ref. [9], eqs. (7) generalize the time-dependent pairing eqs. [17,18], by including two mixing mechanisms, pertaining to the Coriolis and to the Landau-Zener interactions. The first one is managed by the rotational coupling $\langle \Omega', m' | j_\pm | \Omega, m \rangle$ which acts between states that differ by one unit in Ω. The second one is ruled by the interactions $h_{\Omega,m',m}$ that appear in the avoided crossing regions.

The energies of the many-body Hamiltonian H are

$$E_{\Omega,m} = \langle \varphi_{IM\Omega m} | H | \varphi_{IM\Omega m} \rangle$$
$$= 2 \sum_{(\Omega',m') \neq (\Omega,m)} \mid v_{\Omega',m'(\Omega,m)} \mid^2$$
$$\times (\epsilon_{\Omega',m'} - \lambda) + (\epsilon_{\Omega,m} - \lambda)$$
$$- \frac{|\Delta_{\Omega,m}|^2}{G} - G \sum_{(\Omega',m') \neq (\Omega,m)} \mid v_{\Omega',m'(\Omega,m)} \mid^4 \quad (10)$$

for the seniority state (Ω, m), and those due to the external rotations are

$$E^R_{I,\Omega} = \left\langle \varphi_{IM\Omega m} \left| \frac{\hbar^2}{2J} \left(I^2 - j_z^2 \right) \right| \varphi_{IM\Omega m} \right\rangle$$
$$= \frac{\hbar^2}{2J} \left(I(I+1) - \Omega^2 \right), \quad (11)$$

where $|\varphi_{IM\Omega m}\rangle$ are wave functions of the serie (5). Both collective energies intervene in eqs. (7).

The essential solutions of eqs. (7) are the amplitudes $c_{\Omega,m}$. The system is solved from the ground state up to the scission configuration. The values $|c_{\Omega,m}|^2$ at scission gives the probabilities to find the system in the seniority-one configurations (Ω, m). Each seniority-one configurations represent an excited state in which an unpaired nucleon is located on the single-particle level (Ω, m) and $|c_{\Omega,m}|^2$ can be associated as a spectroscopic factor.

Results. – The α-decay of ^{211}Bi is investigated within the macroscopic-microscopic method. The liquid drop part of the deformation energy is obtained with the Yukawa plus exponential model, extended for binary systems with different charge densities [19,20]. The shell and pairing effects are obtained with the Strutinsky prescriptions [21]. A smooth transition between the shell and pairing effects of the parent nucleus to those of both individual nuclei is realized in the scission region where the distance between the centers of the fragments is about 9 fm, as already made for the α-decay of ^{296}Lv in ref. [22]. If the number of single-particle levels in one fragment is too small to apply the Strutinsky procedure, the shell and pairing effects are set to zero, as described in ref. [23]. The collective inertia and the momentum of inertia are obtained within the cranking model [24]. The nuclear system is characterized by some collective coordinates that vary in time leading to a split of the parent nucleus leading to a daughter ^{207}Tl and to an α-cluster, considered as two tangent spherical bodies. Our two-center nuclear shape parametrization is characterized by five degrees of freedom [12], namely the elongation R that denotes the distance between the centers of the nascent fragments, the necking, the two deformations of the fragments and the mass-asymmetry parameter. This shape parametrization is given by two collinear ellipsoids smoothly joined by an intermediate surface. This intermediate surface is obtained by rotating an arc of circle around the axis of symmetry. The fission path was obtained by using the last action principle, as described in ref. [21]. The adiabatic potential barrier V, the effective mass B and the momentum of inertia J, calculated along the least action trajectory are displayed in fig. 1. The nuclear system behaves as a fission process in the initial stage of the disintegration, that is up to $R \approx 3$–4 fm. The internal structure is reorganized and the stabilizing shell and pairing effects are greatly reduced. A first barrier of about 5 Mev is obtained. In the region of the second minimum of the fission barrier, the α-decay path bifurcates to very large mass

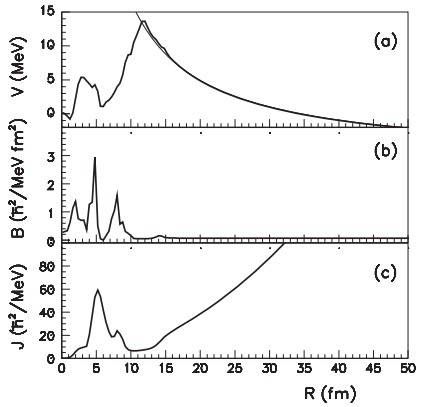

Fig. 1: (a) Potential energy V as a function of the elongation R, normalized with a zero-point vibration energy of 0.5 Mev, is plotted with a thick line. The external Coulomb interaction obtained with the formula $V_C = -Q + 1.43992\frac{Z_1 Z_2}{R}$ (Mev) (R being in fm units) is displayed with a thin line. The Q-value is 6.7503 Mev [25]. (b) Effective mass B along the superasymmetric fission path. (c) Momentum of inertia J.

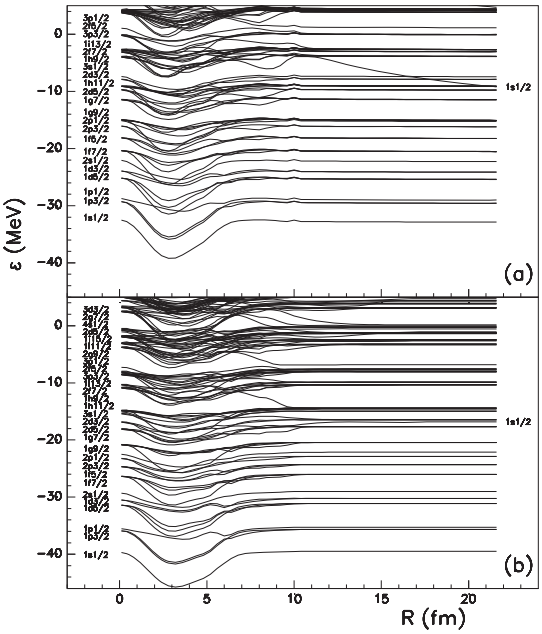

Fig. 2: Single-particle energies ϵ as a function of the internuclear distance R for proton and neutron in panels (a) and (b), respectively. The single-particle level of the α-cluster is marked on the right.

asymmetries. A small peak around $R = 5$ fm locates the region of the bifurcation. The potential barrier evidences a molecular minimum for an elongation R compatible to the scission configuration. This minimum was explained in the previous references [22,26] as the occurrence of the daughter strong shell effects in the final state. It should be noticed that at the same elongation, a deep potential pocket was also remarked in the Pb-He interaction potential in investigations based on effective nucleon-nucleon interactions [27,28]. The effective mass B has fluctuating values. The high values of the effective mass comprised in the interval $R = [1\text{–}6]$ fm are due mainly to variations of the mass asymmetry parameter, while the peak around $R = 8$ fm reflects the rapid variation of the necking. For values larger than $R = 10$ fm, the effective mass stabilizes to a value consistent with the reduced mass. The momentum of inertia J has large values at the beginning of the α-decay process, where the shapes of the system possess reflection symmetry, and reaches the values that correspond to a two-bodies system in the external region. A similar behavior was observed in ref. [29].

Along the fission path, the ingredients required to solve eqs. (7) are calculated within the Woods-Saxon two-center shell model. The model provides the single-particle energies $\epsilon_{\Omega,m}$, and the associated wave functions. From the single-particle level scheme it is possible to identify the avoided levels crossing regions and their interactions $h_{\Omega,m,m'}$ [30]. The system being axial symmetric, the good quantum numbers of the embedded wave functions are the projection of the intrinsic spin Ω on this axis of symmetry. The matrix elements of the angular momenta are calculated with the two-center shell model wave functions. The collective energies are given by eqs. (10) and (11). By using the cranking approach we are able to determine the momentum of inertia J. Now, the coupled channel system (7) can be solved from the parent nucleus initial configuration up to the formation of the alpha particle. The initial conditions are the BCS amplitudes of the ground state of ^{211}Bi, having the total spin $I = 9/2$, for a unpaired nucleon located in the shell $2g_{9/2}$ with spin projection $\Omega = 1/2$.

The single-particle diagrams are represented in fig. 2. Asymptotically, the single-particle energies of the daughter and the α-particle are determined by the solutions of the appropriate Woods-Saxon potentials and are superimposed. In the initial state, $R \approx 0$ fm, the unpaired proton is located on the state $1h_{9/2}$. At scission, $R \approx 10$ fm, the unpaired proton should be retrieved on the state $3s_{1/2}$, to reproduce the ^{207}Tl daughter ground state. By analyzing fig. 2, it can be noticed that a single-particle level with the spin projection $\Omega = 1/2$ emerges from the shell $1h_{9/2}$ of the parent, in order to be ejected in the alpha cluster. This single-particle level is marked on the right with its spectroscopic notation. The α-decay process can occur if the unpaired proton emerging from the state $\Omega = 1/2$, $1h_{9/2}$ is joined by another proton of the nucleus to form a Cooper pair, and both escape outside. This mechanism can be realized if another proton located on a different single-particle level skips to the α-single-particle level during the deformation of the parent nucleus. Such events can be obtained as a result of the Landau-Zener promotion mechanism produced in avoided levels crossing regions. By investigating fig. 2, one expected that at the energy $\epsilon \approx -7$ Mev and $R \approx 8$ fm an avoided crossing level is produced. Here, two-single particle levels characterized by the same spin projection $\Omega = 1/2$, emerging from orbitals $1h_{9/2}$ and $3s_{1/2}$ seem to display a pattern characteristic of an avoided levels crossing region.

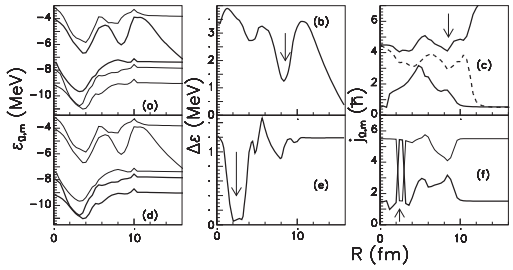

Fig. 3: (a) Five single-particle levels with $\Omega = 1/2$ are plotted. The levels that emerge from $1h_{9/2}$ and $3s_{1/2}$ are plotted with thick lines. (b) The energy difference $\Delta\epsilon$ between the levels plotted with thick lines. An arrow locates a fictitious avoided levels crossing region. (c) The intrinsic angular momenta obtained from the equality $j_{\Omega,m}(j_{\Omega,m}+1) = \langle\Omega, m|j^2|\Omega, m\rangle$ belonging to the thick-line levels of panel (a) are plotted with full curves. These angular momenta are computed from the center of mass of the whole nuclear system. The intrinsic angular momentum corresponding to the level emerging from the spherical shell $I = \frac{9}{2}\hbar$ does not intersect with that of the level emerging from the spherical shell $I = \frac{1}{2}\hbar$. The dashed line gives the intrinsic angular momentum of the level that emerges from $1h_{9/2}$ calculated from the center of mass of the nascent α-particle. The angular momentum reaches the value $\frac{1}{2}\hbar$ if it is calculated from the center of mass of the α cluster. (d) The single-particle levels emerging from $2d_{3/2}$ and $1h_{11/2}$ are plotted with thick-lines. (e) The difference between the values of the thick-line single-particle levels plotted in panel (d). A real avoided levels crossing region is identified with an arrow. (f) The intrinsic angular momenta of the levels emerging from $I = \frac{11}{2}\hbar$ and $I = \frac{3}{2}\hbar$ intersect in the avoided levels crossing region marked with an arrow.

In a true avoided levels crossing region, the levels should exchange their characteristics. For example in atomic physics, a pure polar electron state can become homopolar after the passage of an avoided crossing, as remarked by Zener [11]. To be certain that one had to do with an avoided levels crossing region, one had to check that some features of the states change after the passage through the avoided levels crossing region. In this respect, the energy variation and the intrinsic angular momenta of the $\Omega = 1/2$ levels emerging from $1h_{9/2}$ and $3s_{1/2}$ are compared in fig. 3, panels (a), (b), and (c). But, in the region of the expected avoided levels crossing, the intrinsic angular momenta behave as independent. That means, in this region, no avoided levels crossing is produced. Consequently, the single-particle levels located above and below the energy gap are not coupled by the Landau-Zener effect. Therefore, the fine-structure explanation should rely on promotion mechanisms due mainly to the Coriolis coupling. For a comparison purpose, the behavior produced in a real avoided levels crossing region is displayed in fig. 3, panels (d), (e) and (f).

The behavior of the angular-momentum matrix elements should be investigated. In fig. 4, one plots the matrix elements $\hbar^2\langle\Omega+1, m'|j_+|\Omega, m\rangle/(2J)$ between the states $\Omega = 1/2$ emerging from $2f_{7/2}$, $1h_{9/2}$, $3s_{1/2}$, $2d_{3/2}$,

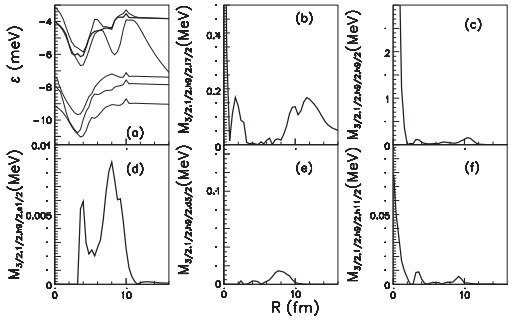

Fig. 4: (a) Single-particle levels with $\Omega = 1/2$ emerging from the spherical states $2f_{7/2}$, $1h_{9/2}$, $3s_{1/2}$, $2d_{3/2}$, $1h_{11/2}$ are plotted with thin curves. These states are ordered for descending energies. A level $\Omega = 3/2$ emerging from $1h_{9/2}$ is plotted with a thick line. The matrix elements $M_{\Omega+1,\Omega,m',m} = \hbar^2\langle\Omega+1, m'|j_+|\Omega, m\rangle/(2J)$ with $\Omega + 1 = 3/2$, $m' = 1h_{9/2}$ are displayed in panels (b) for $m = 2f_{7/2}$, (c) for $m = 1h_{9/2}$, (d) for $m = 3s_{1/2}$, (e) for $m = 2d_{3/2}$, and (f) for $m = 1h_{11/2}$.

$1h_{11/2}$ and the state $\Omega = 3/2$ emerging from the state $1h_{9/2}$. The coupling between the states $(\Omega = 3/2, 1h_{9/2})$ and $(\Omega = 1/2, 1h_{9/2})$ displayed in panel (c) is very large for small internuclear distances R, because of the huge values of the rotational parameter $\hbar^2/(2J)$ for spherical nuclei. That is, a strong Coriolis coupling is produced between the single-particle levels of the same shell. Large values of the interactions are also obtained when the single-particle levels intersect. For example in panel (b) this behavior is evidenced between the states $(\Omega = 3/2, 1h_{9/2})$ and $(\Omega = 1/2, 2f_{7/2})$ at $R = 2$ fm and 10 fm. Successive Coriolis couplings between different states can populate the α-single-particle level with a pair. The probabilities to obtain different seniority-one configurations can be calculated with our system of microscopic equations of motion.

In order to solve the equations of motion, one selected the single-particle levels with spin projection $\Omega = 1/2$ emerging from $2f_{7/2}$, $1h_{9/2}$, $3s_{1/2}$, $2d_{3/2}$, $1h_{11/2}$, the levels with spin $\Omega = 3/2$ emerging from $2f_{7/2}$, $1h_{9/2}$, $2d_{3/2}$, $1h_{11/2}$, the levels with $\Omega = 5/2$ and $7/2$ emerging from $2f_{7/2}$, $1h_{9/2}$, $1h_{11/2}$, and the level with $\Omega = 9/2$ emerging from $1h_{11/2}$. In total 16 single-particle levels, each of them corresponding to a seniority-one configuration. The real avoided levels crossing regions were identified between adjacent levels with the same spin projection Ω. The same internuclear distance velocity $v = \dot{R} = 2 \times 10^4$ fm/fs was used to solve the equations as in ref. [9].

It should be noted that the equations of motion used in ref. [9] for the ^{211}Po alpha decay differ from those used in this work, In the case of ^{211}Po, the equations were solved for the neutron single-particle diagram. In this case, the energy of the α-single-particle level is much lower than the Fermi energy of the whole system. That is, the BCS probability of occupation of the α-level is essentially unity. In the present work, the α-single-particle level is located in the Fermi region. That means, the BCS occupation

Table 1: The initial (parent nucleus) and final (daughter nucleus) orbitals of the single-particle levels selected in the region of the Fermi energy, their spin projection Ω, the square of the amplitudes of the seniority-one configuration in the final state $|c_{\Omega,m}|^2$, the penetrability of the external barrier $P^b_{\Omega,m}$, and the excitation energies of the daughter nucleus $\Delta E_{\Omega,m}$.

Initial state m	Final state	Ω ($\hbar$)	$\lvert c_{\Omega,m}\rvert^2$	$P^b_{\Omega,m}$	$\Delta E_{\Omega,m}$ (Mev)
$2f_{7/2}$	$1h_{9/2}$	1/2	7.735×10^{-2}	1.90×10^{-74}	3.892
$1h_{9/2}$	$1s_{1/2}$ (α)	1/2	4.700×10^{-2}		
$3s_{1/2}$	$3s_{1/2}$	1/2	3.599×10^{-8}	2.66×10^{-36}	0
$2d_{3/2}$	$2d_{3/2}$	1/2	3.414×10^{-8}	7.17×10^{-39}	0.379
$1h_{11/2}$	$1h_{11/2}$	1/2	5.070×10^{-10}	1.55×10^{-53}	2.262
$2f_{7/2}$	$2f_{7/2}$	3/2	0.3951	2.45×10^{-92}	4.833
$1h_{9/2}$	$1h_{9/2}$	3/2	3.787×10^{-3}	2.49×10^{-74}	3.892
$2d_{3/2}$	$2d_{3/2}$	3/2	1.647×10^{-6}	7.85×10^{-39}	0.379
$1h_{11/2}$	$1h_{11/2}$	3/2	3.253×10^{-5}	2.02×10^{-53}	2.262
$2f_{7/2}$	$2f_{7/2}$	5/2	0.3817	2.89×10^{-92}	4.833
$1h_{9/2}$	$1h_{9/2}$	5/2	8.042×10^{-2}	4.08×10^{-74}	3.892
$1h_{11/2}$	$1h_{11/2}$	5/2	1.030×10^{-6}	3.32×10^{-53}	2.262
$2f_{7/2}$	$2f_{7/2}$	7/2	8.211×10^{-3}	3.81×10^{-92}	4.833
$1h_{9/2}$	$1h_{9/2}$	7/2	6.380×10^{-3}	7.24×10^{-74}	3.892
$1h_{11/2}$	$1h_{11/2}$	7/2	7.410×10^{-9}	5.812×10^{-53}	2.262
$1h_{11/2}$	$1h_{11/2}$	9/2	7.805×10^{-10}	9.28×10^{-53}	2.262

probability of the α-single-particle level should be about 1/2 during the deformation of the parent nucleus. By introducing the condition of projection of the number of particles, the BCS probability for the α-level reached a number close to unity when the equations of motion are solved for different seniority-one configurations. The values obtained for the BCS probability of occupation for the α-single-particle level at scission range between 0.997 and 1. The initial condition is considered $c_{\Omega,m}=1$ for $\Omega=1/2$ and $m=1h_{9/2}$, other values of the seniority-one wave function amplitudes being considered 0. The initial occupation/vacancy amplitudes for the single-particle levels of each seniority-one configuration were obtained within the BCS theory. The equations of motion are solved up an internuclear distance $R=10\,\mathrm{fm}$, corresponding to scission. The resulting probabilities of realization of the seniority-one configurations $|c_{\Omega,m}|^2$ are given in table 1. It can be noticed that $\sum_{\Omega,m}|c_{\Omega,m}|^2=1$, that is, the condition of conservation of the probability is fulfilled.

Once the scission point is reached, the alpha emission proceeds by penetrating a potential barrier. The lowest energy potential barrier corresponds to the seniority-one configurations in which the ^{207}Tl daughter nucleus is in the ground state, that is for $\Omega=1/2$ and $m=3s_{1/2}$. For the excited states (Ω,m) of the daughter, the barrier increases with the specialization energy $\Delta E_{\Omega,m}=E_{\Omega,m}-E_{1/2,3s_{1/2}}$, the collective energy $E_{\Omega,m}$ being obtained with eq. (10). These differences were calculated for the daughter nucleus and are presented in table 1. After scission $\Delta E_{\Omega,m}$ behave as constants. For a specific spherical orbital, the energies $E_{\Omega,m}$ are degenerated in the values of Ω. The collective rotational term $E^R_{I,\Omega}(R)$ ($I=9/2$), given by eq. (11) should also be added to the potential barrier, and the degeneration disappears. The penetrabilities P_{Ω,m^b} are calculated with the WKB formalism:

$$P^b_{\Omega,m}=\exp\left\{-\frac{2}{\hbar}\int_{R_i}^{R_{\Omega,m}}\sqrt{2B(R)V_t(R)}\mathrm{d}R\right\},\qquad(12)$$

where $V_t(R)=V(R)+E_{\Omega,m}-E_{1/2,3s_{1/2}}+E^R_{I,\Omega}(R)$. The integral is calculated from the ground state $R_i=1$ fm up to the scission point of each channel $R_{\Omega,m}$. The theoretical values of the barrier penetrabilities of each final state are given in table 1. The yields $Y_{\Omega,m}$ of these channels are proportional to their penetrabilities and their probability to be obtained, that is $Y_{\Omega,m}\propto|c_{\Omega,m}|^2P^b_{\Omega,m}$. The yield for transitions to the final state m is $Y_m=\sum_\Omega Y_{\Omega,m}$. The yields in percents, that correspond to transitions to the final states of the ^{207}Tl daughter, are obtained by using the normalization $N=Y_{2f_{7/2}}+Y_{1h_{9/2}}+Y_{3s_{1/2}}+Y_{2d_{3/2}}+Y_{1h_{11/2}}$. These normalized yields are 87.901%, 12.098%, 6.35×10^{-15}%, 4.87×10^{-32}%, and 1.92×10^{-49} % to the states of the daughter nucleus $3s_{1/2}$, $2d_{3/2}$, $1h_{11/2}$, $1h_{9/2}$ and $2f_{7/2}$, respectively. The theoretical results agree with the experimental findings of ref. [31]. Experimentally, the fine structure is characterized by the intensities 83.77%, 16.23% and <0.0019% [31] to the single-particle states $1/2^+$, $3/2^+$ and $11/2^-$ of the ^{207}Tl daughter, respectively.

Conclusion. – Most treatments of α-decay consider that the α-particle is born on the surface of the nucleus [32–34]. Amplitudes of preformation for ^{211}Bi were calculated in refs. [35,36]. But, for a long time it was invoked that a similarity exists between the fission penetrability of the inner barrier in α-decay and the preformation probability [37,38]. Phenomenological treatments were performed and this fission barrier was never determined effectively with fission models. In fission models, at least the modification of the nuclear structure with the help of shell and pairing effects must be taken into account. In the best achievements, the barrier in the overlap region was calculated within the liquid drop model, and the structure effects were considered in a phenomenological way, by adding empirically a correction that match the Q-value asymptotically. In this way, the height of the external barrier is fixed, as it happens in the phenomenological theory of α-decay. In less sophisticated approaches, the inner barrier is fitted with a simple function, or, only the influence of the proximity potential at scission served to improve the shape of the potential barrier. By including the zero-point vibration energy on an empirical way, it was possible to obtain a half-life systematic. These phenomenological models cannot find the causes of the fine-structure phenomenon, which are due to microscopic effects.

In a fission-like theory, as the present treatment, the α-particle is born on the surface of the nucleus by modifying the collective coordinates of the nuclear system, and hence the mean-field potential of all nucleons. A similar concept is given by the dinuclear model, in which the nucleons are transferred gradually from one nucleus to

another [39,40] Such treatments of the α-decay were already performed in refs. [22,26,41,42], but only recently the dynamics was investigated by taking into account the angular coupling [9] in the superfluid model. In the spontaneous fission theory, firstly we need to determine a fragmentation path. This path determine the collective inertia, the deformation energy, together with the rearrangement of the single-particle levels. The calculations of the spectroscopic factors rely on the solution of a system of microscopic equations of motion that take into account the dynamical effects due to the rearrangement of the single-particle levels during the deformation of the parent nucleus. A generalization of the time-dependent pairing equations that includes the radial and the Coriolis couplings was used to determine quantities that have the same meaning as the spectroscopic factors. The ^{211}Bi α-decay fine structure was investigated microscopically and good agreement with experimental findings was obtained. It should be noted that our model suggests that the large value of the yield to the ground state of the daughter is due exclusively to the occurrence of the Coriolis coupling during the deformation of the parent nucleus, corroborated with a large corresponding penetrability. The population of the proton states of the emitted particle is obtained dynamically.

The approach is still limited by some drawbacks. The ground-state configuration of the parent nucleus is constrained by five generalized coordinates while the ground states of both fragments are left with only one deformation parameter, that is the eccentricity. That leads to a weaker description of the ground states of the daughter nuclei and of the α-particle during the penetration of the external barrier. It is also questionable how the sorting of the shell and pairing effects is produced at scission. The issue concerning the pairing was investigated already by using a density-dependent delta interaction model in ref. [26]. Also, the model does not provide information about the radial motion. Similar equations of motion can be deduced for even-even systems. In this case, the trial wave function (5) should be considered as a mixing of seniority-zero and seniority-two states coupled by the dynamical pair breaking effect, analogous to the Landau-Zener mechanism [13]. Matrix elements of $j_{\pm}$ exist between the seniority-one and seniority-two wave functions. Therefore, it is possible to follow a similar approach, but with a more complicated trial wave function.

* * *

This work was supported by the grants of Ministery of Research and Innovation, CNCS-UEFISCDI, project numbers PN-III-P4-ID-PCE-2016-0092 and PN-III-P4-ID-PCE-2016-0014, within PNCDI III.

REFERENCES

[1] Delion D. S., *Theory of Particles and Cluster Emission* (Springer, Berlin) 2010.
[2] Mang H. J., *Phys. Rev.*, **119** (1962) 1069.
[3] Sandulescu A., *Nucl. Phys. A*, **37** (1962) 332.
[4] Ropke G. *et al.*, *Phys. Rev. C*, **90** (2014) 034304.
[5] Ropke G. *et al.*, *J. Low Temp. Phys.*, **189** (2017) 383.
[6] Deng D., Ren Z., Ni D. and Qian Y., *J. Phys. G*, **42** (2015) 075106.
[7] Mirea M., *Eur. Phys. J. A*, **51** (2015) 36.
[8] Delion D. S., Ren Z., Dumitrescu A. and Ni D., *J. Phys. G*, **45** (2018) 053001.
[9] Mirea M., *Phys. Rev. C*, **96** (2017) 064607.
[10] Landau L. D., *Phys. Z. Sowjet.*, **46** (1932) 46.
[11] Zener C., *Proc. R. Soc. A*, **137** (1932) 696.
[12] Mirea M., *Phys. Rev. C*, **78** (2008) 044618.
[13] Mirea M., *Phys. Lett. B*, **680** (2009) 316.
[14] Bohr A. and Mottelson B. R., *Nuclear Structure*, Vol. **II**: *Nuclear Deformations* (World Scientific, Singapore) 1998.
[15] Mirea M., *Phys. Lett. B*, **717** (2012) 252.
[16] Mirea M., *Phys. Rev. C*, **89** (2014) 034623.
[17] Koonin S. E. and Nix J. R., *Phys. Rev. C*, **13** (1976) 209.
[18] Blocki J. and Flocard H., *Nucl. Phys. A*, **273** (1976) 45.
[19] Moller P., Nix J. R., Myers W. D. and Swiatecki W. J., *At. Data. Nucl. Data. Tables*, **59** (1995) 185.
[20] Mirea M. *et al.*, *Eur. Phys. J. A*, **11** (2001) 59.
[21] Brack M. *et al.*, *Rev. Mod. Phys.*, **44** (1972) 320.
[22] Sandulescu A., Mirea M. and Delion D. S., *EPL*, **101** (2013) 62001.
[23] Mirea M., Sandulescu A. and Delion D. S., *Nucl. Phys. A*, **870-871** (2011) 23.
[24] Mirea M., *J. Phys. G*, **43** (2016) 105103.
[25] Wang M. *et al.*, *Chin. Phys. C*, **36** (2012) 1603.
[26] Mirea M., *Eur. Phys. J. A*, **51** (2015) 36.
[27] Adamian G. G., Antonenko N. V., Lenske H., Tolokonnikov S. V. and Saperstein E. E., *Phys. Rev. C*, **94** (2016) 054309.
[28] Xu C. *et al.*, *Phys. Rev. C*, **95** (2017) 061306.
[29] Mirea M. and Sandulescu A., *Proc. Rom. Acad. Ser. A*, **19** (2018) 201.
[30] Greiner W., Park J. Y. and Scheid W., *Nuclear Molecules* (World Scientific, Singapore) 1995.
[31] Kondev F. G. and Lalkovski S., *Nucl. Data Sheets*, **112** (2011) 707.
[32] Anghel C. I. and Silisteanu I., *Phys. Rev C*, **95** (2017) 034611.
[33] Anghel C. I. and Silisteanu I., *Rom. J. Phys.*, **62** (2017) 303.
[34] Adel A. and Alharbi T., *Nucl. Phys. A*, **975** (2018) 1.
[35] Fliessbach T., Mang H. G. and Rasmussen J. O., *Phys. Rev. C*, **13** (1976) 1318.
[36] Kadmensky S. G., *Z. Phys. A*, **312** (1983) 113.
[37] Poenaru D. N. and Greiner W., *J. Phys. G*, **17** (1991) S443.
[38] Zdeb A., Warda M. and Pomorski K., *Phys. Rev C*, **87** (2013) 024308.
[39] Volkov V. V., *Phys. Rep.*, **44** (1978) 93.
[40] Volkov V. V., *Nuclear Shells-50 Years* (World Scientific, Singapore) 2000.
[41] Mirea M., *Phys. Rev. C*, **63** (2001) 034603.
[42] Mirea M., Budaca R. and Sandulescu A., *Ann. Phys. (N.Y.)*, **380** (2017) 154.